

Oxygen bridged Homobinuclear Mn(II) compounds with Anthranilic acid: Theoretical calculations, oxidation and catalase activity

Esra Su^{1,2}  | Alaettin Guven²  | Ibrahim Kani²

¹Department of Chemistry, Faculty of Science & Letters, Istanbul Technical University, Maslak, 34469, Istanbul, Turkey

²Department of Chemistry, Faculty of Science, Anadolu University, 26470 Eskisehir, Turkey

Correspondence

Ibrahim Kani, Department of Chemistry, Faculty of Science, Anadolu University, 26470, Eskisehir, Turkey.
Email: ibrahimkani@anadolu.edu.tr

Funding information

The Scientific and Technological Research Council of Turkey (TUBITAK), Grant/Award Number: 113Z303; Anadolu University (BAP), Grant/Award Number: 1406F390

Two new homobinuclear manganese compounds with mixed ligands, $[\text{Mn}_2(\mu_{1,1}\text{-}2\text{-NH}_2\text{C}_6\text{H}_4\text{COO})_2(\text{phen})_4](\text{ClO}_4)_2(\text{CH}_3\text{OH})$ (**1**), and $[\text{Mn}_2(\mu_{1,3}\text{-}2\text{-NH}_2\text{C}_6\text{H}_4\text{COO})_2(\text{bipy})_4](\text{ClO}_4)_2$ (**2**) ($\text{NH}_2\text{C}_6\text{H}_4\text{COOH}$ = anthranilic acid, bipy = 2,2'-bipyridine, phen = 1,10-phenanthroline) were synthesized and thoroughly characterized by elemental analysis, IR, UV and single crystal X-ray crystallography. X-ray structure analysis shows that in the mono- and bidentate carboxylate bridged compounds, Mn–Mn distances of **1** and **2** are 3,461 Å, and 4,639 Å, respectively. The energy of the compounds was determined with a DFT (Density Functional Theory) calculation on B3LYP/6-31G(d,p) optimized geometry by using the B3LYP/6-31G(d,p) basis set. These compounds act as biomimetic catalyst and show catalase-like activity for the hydrogen peroxide dismutation at room temperature in different solvents with remarkable activity (TOF, Turnover frequency = mol of subst./mol of cat. × time) up to 12640 h⁻¹ with **1**, and 17910 h⁻¹ with **2** in Tris–HCl buffer). Moreover, the catalytic activity of **1** and **2** has been studied for oxidation of alcohols (cinnamyl alcohol, benzyl alcohol, cyclohexanol, 1-octanol and 1-heptanol) and alkenes (cyclohexene, styrene, ethyl benzene, 1-octene and 1-hexene) in a homogeneous catalytic system consisting *t*-butylhydroperoxide (TBHP) as an oxidant in acetonitrile. Both compounds exhibited very high activity in the oxidation of cyclohexene to cyclohexanone (~80% selectivity, ~99% conversion in 1 h, TOF = 243 h⁻¹ and 226 h⁻¹) and cinnamyl alcohol to cinnamaldehyde (~64% selectivity) as the main product with very high TOF value (9180 h⁻¹ and 13040 h⁻¹ in the first minute of reaction) (~100% conversion in 0.5 h) with TBHP at 70 °C in acetonitrile, for **1** and **2**, respectively.

KEYWORDS

alcohol, alkenes, catalase activity, catalysis, manganese, oxidation

1 | INTRODUCTION

Aerobic respiration products can be generated by reactive oxygen species (ROS) such as the superoxide anion,

hydroxyl radical and hydrogen peroxide. These ROS are associated with numerous pathological conditions, including atherosclerosis, ischemic, cancer and Alzheimer's diseases as well as aging.^[1] Also, hydrogen

peroxide, which is among the reactive oxygen species, can be converted into the reactive hydroxyl radical and therefore is able to damage a variety molecules within a cell, leading to oxidative stress and cell death via transition metals such as Fe^{2+} and Cu^{2+} by Fenton chemistry.^[2] All living cells therefore use elaborated organized mechanisms to control the level of ROS by using metalloenzymes such as the superoxide dismutase (SODs) and catalases (CATs). Manganese-dependent CATs has been identified in three bacterial organisms: *Lactobacillus plantarum*,^[3] *Thermus thermophilus*^[4] and *Thermoleophilum album*.^[5] Manganese-dependent CATs are catalyze disproportionation of H_2O_2 into H_2O and O_2 ($2\text{H}_2\text{O}_2 \rightarrow 2\text{H}_2\text{O} + \text{O}_2$) by using a $[\text{Mn}_2(\mu\text{-O}/\text{OH}/\text{H}_2\text{O})_2(\mu\text{-RCOO})]$ structural unit which contains one carboxylate bridge and one or two bridging O-ligands from the solvent (oxo, hydroxo, or aqua)^[6] and protect biological systems against oxidative damage caused by toxic metabolites (hydrogen peroxide) formed during aerobic metabolism. They can exist in at least four different oxidation states: a reduced Mn^{II}_2 form, a mixed valence $\text{Mn}^{\text{II}}\text{Mn}^{\text{III}}$ form, an oxidized Mn^{III}_2 form and a superoxidized $\text{Mn}^{\text{III}}\text{Mn}^{\text{IV}}$ form.^[7] However, only Mn^{II}_2 - Mn^{III}_2 oxidation states are able to catalyze the dismutation of hydrogen peroxide at extremely high rates.

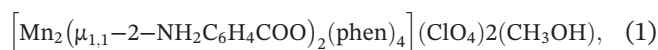
During the past two decades, a wide variety of binuclear manganese compounds have been synthesized to mimic structural features.^[8] However, the best mimic model has quite slow catalase activity compared to the enzyme and therefore new type of catalase mimic manganese-dependent compounds are attracted much attention in recent years. In addition, the use of inorganic-organic hybrid compounds as a catalyst for the oxidation of alcohols and alkenes is of current interest, and some efficient metal organic frameworks used as a catalysts have been reported.^[9] However, most metal-containing catalysts that are used in industry are very expensive and need the development of a cheaper, effective and environmentally friendly catalytic system. As a continuation of our catalytic research,^[10] the purpose of this work was synthesize new manganese compounds with carboxylate and nitrogenous base ligands as oxidation catalyst. Here, we report the synthesis, crystallographic structure and physical properties of carboxylate bridged homobinuclear compounds of Mn(II), $[\text{Mn}_2(\mu_{1,1}\text{-}2\text{-NH}_2\text{C}_6\text{H}_4\text{COO})_2(\text{phen})_4](\text{ClO}_4)_2(\text{CH}_3\text{OH})$ (**1**), and $[\text{Mn}_2(\mu_{1,3}\text{-}2\text{-NH}_2\text{C}_6\text{H}_4\text{COO})_2(\text{bipy})_4](\text{ClO}_4)_2$ (**2**), (phen = 1,10'-phenanthroline and bipy = 2,2'-bipyridine) and successful application of these compounds as catalyst toward the disproportionation of H_2O_2 and in the oxidation of alcohols and alkenes in different organic solvents. Furthermore, some theoretical calculations are performed with these compounds.

2 | EXPERIMENTAL

2.1 | General

All starting materials and organic solvents were purchased from commercial sources and were utilized as received without further purification. IR spectra were recorded using KBr pellets on a Jasco FT/IR-300E in the range 4000–400 cm^{-1} . C, H, N analysis was performed using a Vario EL III Elemental analyzer. UV-Vis spectra were recorded on a Shimadzu UV-2450 spectrophotometer using quartz cells. The intensity data were collected with using Bruker Smart Apex II single-crystal diffractometer. All calculations were performed using the SHELXTL program.

2.2 | Synthesis of compounds



$\text{Mn}(\text{ClO}_4)_2 \cdot 6\text{H}_2\text{O}$ (401 mg; 1.11 mmol) in methanol (10 ml) was added to a 5-ml methanol solution of anthranilic acid (152 mg; 1.11 mmol). The pH of anthranilic acid was adjusted to 7 with 5.2 ml NaOH solution (0.245 M). The white cloudy solution was stirred for 2 h, then the 5.0-ml methanol solution of phen (200 mg; 1.11 mmol) was added to this solution. A yellow suspension formed immediately. The mixture was refluxed during 5 h at 50 °C, and the yellow solution was filtrated off and allowed to stand at room temperature for a few days. After standing, a crystalline yellow solid was filtered off and washed with diethylether (205 mg; Yield: 55.4% m.p.: 257 °C; soluble in polar organic solvents, Anal. Cal. for $\text{C}_{63}\text{H}_{48}\text{Cl}_2\text{Mn}_2\text{N}_{10}\text{O}_{13}$ (1333.84 g) C, 56.73; H, 3.63; N, 10.50%, Found: C, 54.20; H, 3.31; N,10.35%) (Significant IR bands (KBr, ν cm^{-1}) (s, strong; m, medium; w, weak): 3458w $\nu\text{N-H}$, 1578 m $\nu\text{C} = \text{N}$; 1624 m $\nu\text{COO}_{\text{asym}}$; 1426 m $\nu\text{COO}_{\text{sym}}$; 1519 m $\nu\text{C} = \text{N-C} = \text{C}_{\text{sym}}$; 1147 m $\nu\text{O-H}$; 1084s $\nu\text{C-O}$; 846 m $\nu\text{C-N}$; 723 m $\nu\text{Mn-O-Mn}_{\text{sym}}$; 622 m $\nu\text{Mn-O-Mn}_{\text{asym}}$) UV λ_{max} nm (CH_3CN): 202, 227, 270



NaOH (4 ml; 0.245 M) in 10 ml of methanol was added dropwise to a stirred solution of $\text{Mn}(\text{ClO}_4)_2 \cdot 6\text{H}_2\text{O}$ (350 mg; 0.98 mmol) and anthranilic acid (132 mg; 0.98 mmol) in 20 ml of methanol at 50 °C. The mixture (pH = 7) was stirred for 2 h, and a yellow suspension formed immediately. Then 5.0-ml methanol solution of bipy (150 mg; 0.98 mmol) was added to the mixture, and

a yellow solution formed. The solution was refluxed during 5 h at 50 °C and filtrated off. Crystals were obtained by slow diffusion and washed with diethyl ether (125 mg; Yield: 42.3%, d.p.: 243 °C, soluble in polar organic solvents; Anal. Cal. for C₅₄H₄₄Cl₂Mn₂N₁₀O₁₂ (1205.77 g) C, 53.79; H, 3.68; N, 11.62% Found: C, 53.46; H, 3.65; N, 11.61%) (Significant IR bands (KBr, ν cm⁻¹) (s, strong; m, medium; w, weak): 3416w ν N-H, 1575 m ν C = N; 1597 m ν COO_{asym}; 1440 m ν COO_{sym}; 1474s ν C = N-C = C_{sym}; 1087s ν C-O; 846 m ν C-N; 737 m ν Mn-O-Mn_{sym}; 623 m ν Mn-O-Mn_{asym}) (UV λ_{\max} nm (CH₃CN): 198, 242, 294

2.3 | X-ray crystallographic analysis

Yellow color crystals of the manganese compounds **1** and **2** were mounted on a glass fiber and diffraction data for the complexes collected with Bruker AXS APEX CCD diffractometer equipped with a rotation anode at 100(2), 293(2) and 296(2) K, respectively using graphite monochromated Mo K α radiation at $\lambda = 0.71073$ Å in the incident beam. Unit cell dimensions were determined by least-squares refinement of the complete data set. The data reduction was performed with the Bruker SMART program package.^[11] The relevant crystal data are summarized in SP2. The structures were solved by direct methods and the non-hydrogen atoms were located through subsequent difference Fourier syntheses.^[12] Structure solution was found with the SHELXS-97 package using the direct methods and were refined SHELXL-97^[13] against F² using first isotropic and later anisotropic thermal parameters for all non-hydrogen atoms. Hydrogen atoms were added to the structure model at calculated positions. The molecular drawing was obtained using MERCURY.^[14] Geometric calculations were performed with PLATON.^[15]

2.4 | Computational methods

All calculations were carried out by 64-bit Gaussian 09 software^[16] implemented on Linux OpenMandriva. The structures investigated were optimized before computing energies, IR and UV spectra by using B3LYP density functional and 6-31G(d,p) basis set. This level of theory gives a reasonable result which are generally well agreement with the experimental X-ray geometry.^[17] The B3LYP approach includes Becke's three parameter hybrid exchange potential^[18] and the Lee–Yang–Parr correlation functional.^[19]

2.5 | Catalase activity

The catalase activity studies were performed by volumetric determination of the oxygen evolved with a gas-volumetric burette (precision of 0.1 ml). A flask with

a stopcock-equipped gas delivery side tube was connected to a gas-measuring burette. A 30% H₂O₂ aqueous solution (9.7×10^{-3} mol, 1 ml) was added to closed vessels through the rubber septum using a syringe, containing acetonitrile (5.0 ml) solutions of **1** or **2**, and the oxygen evolution was measured volumetrically. The H₂O₂ / catalyst ratio was used as 2500. The catalyst concentration in reaction mixture is 6.47×10^{-4} . The mixture of catalyst and H₂O₂ was stirred at constant temperature in an oil bath. The same procedure was repeated with all compounds in different solvents. The catalytic activity of Mn(ClO₄)₂ toward H₂O₂ disproportion was tested under the similar conditions, as stated above in acetonitrile solution. The volume of oxygen gas was calculated by using the ideal-gas equation.

2.6 | General procedure of the catalytic oxidation experiments

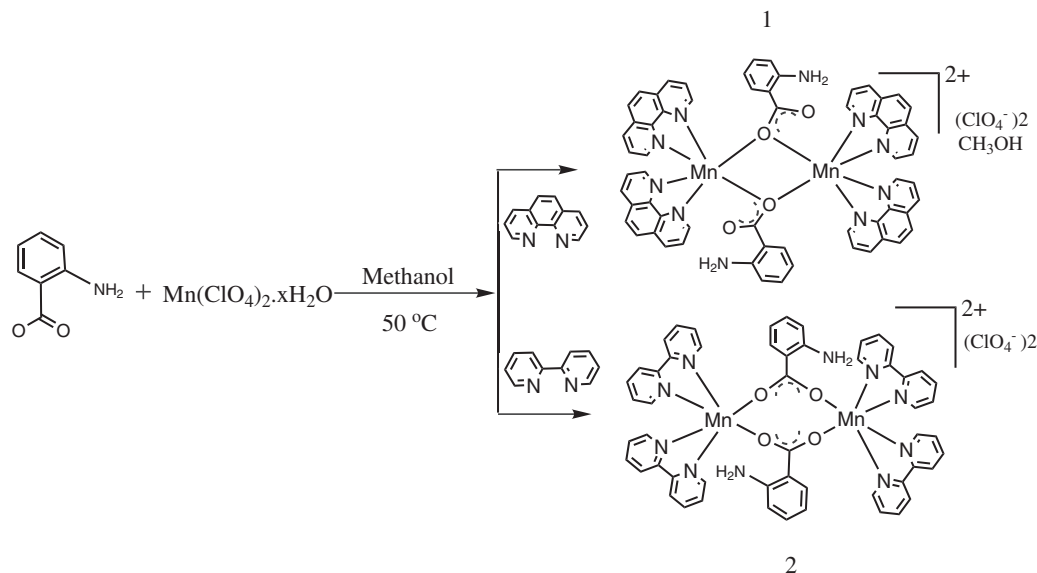
The study of catalytic reactions was performed in 50 ml flasks with a temperature controller unit. 2 ml (1.46×10^{-2} mol) of solution of oxidant was added dropwise to a mixture of substrate and catalyst (~0.5–1%) at 70 °C. The substrate / catalyst ratio was kept constant at 265. The reaction mixture was analyzed at certain time intervals with GC (HP-5 quartz capillary column (30 m \times 0.32 mm \times 0.25 μ m) and a FID detector using nitrogen as the carrier gas (rate of 1.0 ml min⁻¹).

3 | RESULTS AND DISCUSSION

3.1 | Synthesis and characterization of the compounds

The synthesis of compounds is shown in Scheme 1. The observed two strong peaks at ~1426 and ~1626 cm⁻¹ for **2** can be assigned to stretching vibration symmetric and asymmetric carboxylate group, respectively. In the infrared spectrum of compound **2**, the magnitude of separation (~200 cm⁻¹) indicates bidentate ($\mu_{1,3}$) coordination of the carboxylate ion according to Nakamoto's method.^[20] However, in the spectrum of **1**, the bands at 1440 and 1597 cm⁻¹ are assigned to $\nu_{as}(\text{CO}_2)$ and $\nu_{s}(\text{CO}_2)$; the Δ value (157 cm⁻¹) is not as large as expected ($\Delta > 250$ cm⁻¹) for monodentate bridging ($\mu_{1,1}$) modes of benzoate ligation.^[21] This is due to the fact that the carboxylate oxygen (O(6) in Figure 2) not coordinated to Mn(II) is hydrogen bonded to the neighboring groups, giving what can be regarded as a 'pseudo-bridging' arrangement.

X-ray structure analysis was confirm this coordination. The $\nu(\text{N-H})$, $\nu(\text{C} = \text{N})$ and $\nu(-\text{C} = \text{N}-\text{C} = \text{C}-)$ vibrations of rings are observed at 3416; 3458, 1578; 1575



SCHEME 1 Synthesis of **1** and **2**

and $1519; 1474\text{ cm}^{-1}$, for **1** and **2**, respectively. The medium bands at 723 and 623 cm^{-1} may be assigned to stretching vibration asymmetric and symmetric Mn–O–Mn, respectively.^[22] This fact implies the existence of binuclear manganese core. The IR spectra of the compounds are all similar, apart from bands due to vibrations of the N,N ligand and the coordination mode of the carboxylate groups. The bands centered at ~ 1600 , 1498 , 1480 and 1450 cm^{-1} are assigned to the bipy. In the spectrum of **2**, the observed bands at 1120 cm^{-1} and 623 cm^{-1} are assigned to the perchlorate anion.

The UV spectrum of compounds was taken in acetonitrile (SP2). The observed maximum absorptions at $190\text{--}300\text{ nm}$ may be assigned to $\pi\text{--}\pi^*$ transitions of the K band of the benzene rings and the charge transfer band to ligand from metal (MLCT).^[23]

Molar conductivity measurements allowed verification of the stability of compounds and the degree of dissociation of the compounds in studied solutions. Compounds **1** and **2** with perchlorate anions, have Λ_M values close to the expected for 1:2 electrolytes (one cation and two anion) in the solvents: acetonitrile: 296 , methanol: 302 , water; 229 and tirs-HCl buffer: $271\text{ S cm}^2\text{ mol}^{-1}$. Thus, in solution these compounds retain their binuclear structures in solution and also the perchlorate anions are not coordinated to the manganese ions.

3.2 | Crystal structure of compounds

X-ray analysis and spectral data consistent with the structure of the compounds. The structural parameters of **1** and **2** are in agreement with those reported for compounds with the same $[\text{Mn}_2(\mu\text{-O})(\mu\text{-2-RC}_6\text{H}_4\text{CO}_2)_2]^{2+}$

core.^[24] For both compounds, crystallographic data (SP1) and the some selected bond lengths and angles are listed in Table 1.

The crystal structure of **1** shows a homobinuclear cationic complex. The asymmetric unit of complex cation contains one anthranilate and two phen ligands. Two perchlorate anions are located outside as counter ions and one free methanol molecule. The cationic structure is shown in Figure 1(a). The Mn(II) ions are bridged by two carboxylate ligands in a monodentate mode ($\mu_{1,1}$) with Mn \cdots Mn distance of 3.463 \AA and a Mn–O–Mn angle of 105.3° . Binuclear Mn(II) compounds displaying this type of bridging mode are not very common and few compounds reported in the literature similar enough to compare the structural parameters (Table 2).^[25] The structure of **1** presented in this work, together with that published data, represents a Mn(II) complex containing a pure monodentate bridging carboxylate without any apparent interaction of the dangling oxygen with Mn(II). The distance between Mn and the dangling oxygen (O2) is 3.80 \AA which excludes a bonding interaction. The Mn \cdots Mn distance, 3.463 \AA in our case is longer than reported (3.177 \AA)^[25i] (Table 2) and is shorter than 3.53 \AA and 3.59 \AA in the analogous structure^[25a,25f,25g], and is very close the others ($\sim 3.45\text{ \AA}$)^[25a], and can be related to the unusual bridging mode.

Anthranilate anion are in a *trans* position in an asymmetric unit. All phen rings are nearly planar (dihedral angle $\text{N1C12C11N2}\text{--}2.14(3)^\circ$ and $\text{N4C23C24N3}\text{--}1.60(3)^\circ$). The one oxygen of carboxylate groups of two different anthranilate bridge two metal center in mono-bidentate mode. The six coordination of each Mn(II) completed by two chelating phen

TABLE 1 Some selected bond lengths (Å) and angles (°) for compounds **1** and **2**.

1		2	
Mn(1)-O(1)	2,160(10)	Mn(1)-O(5)	2,0867(12)
Mn(1)-O(1)#1	2,193(10)	Mn(1)-O(6)#1	2,1428(12)
Mn(1)-N(2)	2,247(12)	Mn(1)-N(4)	2,2381(15)
Mn(1)-N(3)	2,253(11)	Mn(1)-N(1)	2,2711(15)
Mn(1)-N(1)	2,241(13)	Mn(1)-N(2)	2,2831(15)
Mn(1)-N(4)	2,270(11)	Mn(1)-N(3)	2,3064(15)
O(1)-Mn(1)-O(1)#1	74,6(4)	O(1)-Mn(1)-O(1)#1	74,6(4)
O(1)-Mn(1)-N(2)	96,9(4)	O(1)-Mn(1)-N(2)	96,9(4)
O(1)#1-Mn(1)-N(2)	103,7(4)	O(1)#1-Mn(1)-N(2)	103,7(4)
O(1)-Mn(1)-N(3)	100,6(4)	O(1)-Mn(1)-N(3)	100,6(4)
O(1)#1-Mn(1)-N(3)	95,4(4)	O(1)#1-Mn(1)-N(3)	95,4(4)
N(2)-Mn(1)-N(3)	157,0(4)	N(2)-Mn(1)-N(3)	157,0(4)
O(1)-Mn(1)-N(1)	160,0(4)	O(1)-Mn(1)-N(1)	160,0(4)
O(1)#1-Mn(1)-N(1)	90,0(4)	O(1)#1-Mn(1)-N(1)	90,0(4)
N(2)-Mn(1)-N(1)	74,0(4)	N(2)-Mn(1)-N(1)	74,0(4)
N(3)-Mn(1)-N(1)	93,4(4)	N(3)-Mn(1)-N(1)	93,4(4)
O(1)-Mn(1)-N(4)	90,5(4)	O(1)-Mn(1)-N(4)	90,5(4)
O(1)#1-Mn(1)-N(4)	160,0(4)	O(1)#1-Mn(1)-N(4)	160,0(4)
N(2)-Mn(1)-N(4)	91,1(4)	N(2)-Mn(1)-N(4)	91,1(4)
N(3)-Mn(1)-N(4)	73,9(4)	N(3)-Mn(1)-N(4)	73,9(4)
N(1)-Mn(1)-N(4)	107,2(4)	N(1)-Mn(1)-N(4)	107,2(4)
Mn(1)-O(1)-Mn(4)	105,28(7)		

Symmetry code: #1 -x + 2, -y + 2, -z + 1

ligands. Distortion of octahedral geometry around the Mn(II) ions is observed with Mn-O distances (~2.178 Å) much shorter than the Mn-N distances (~2.295 Å). All distances are in agreement with the reported analogous compounds.^[24,25] In the dimer, both Mn atoms are six-coordinated. As shown in Figure 1(b), the oxygen–oxygen atom distance is 2.644 Å in the ring (R4), which is formed with four atoms (Mn1O1Mn1#O1#). In addition, the close $\pi\cdots\pi$ interaction has been observed between the ring of acid (ring R1, C26-C31) and phen ligands (ring R2, C4C5C6C7C11C12 and ring R3, C16C17C18C19C23C24), 3.654 Å and 4.493 Å, respectively (Figure 1 (b)).

The crystal structure of **2** consists of a homobinuclear cationic complex and two perchlorate anions as a counter ion. The asymmetric unit of complex cation consist of two bipy ligands and one anthranilate anion. The structure of the cationic complex is shown in Figure 2 (a). The two Mn(II) ions are bridged by two anthranilate ligands, in a bidentate *syn-anti* mode ($\mu_{1,3}$) with a Mn \cdots Mn distance of 4.639 Å and a O-Mn-O angle of 98.44°. As shown in

Figure 2 b), the diagonal length, which corresponds to the carbon–carbon atom distance, is 4.235 Å in the ring R8, which is formed with eight atoms (Mn1O6C21O5Mn1O6C21O5). In addition, the $\pi\cdots\pi$ interactions have been observed between the ring of acid (ring R5, C22-C27) and bipy ligands (ring R6, N4C11-C15) and ring R7, N2C6C10), 4.544 Å and 6.320 Å as shown in Figure 2 b).

The six-coordination of each Mn(II) ion is completed by chelation of two bipy ligands with Mn-N distances that range from 2.238 to 2.306 Å. The Mn – O bond distances of the oxo bridges are ~2.087 Å, and the Mn – N distances are ~2.143 Å. The bipy ligands, which are *cis* position to acid, are closer to planarity, as indicated by the N3 – C16 – C15 – C14 and C7 – C6 – C5 – N1 torsion angles, which are –160.12° and 174.68°, respectively. All distances and angles for **2** are in agreement with the reported similar compounds with the same Mn-carboxylate bridged mode.^[24,81,8m,8n,9a,9e,9f]

Both compounds have strong intra- and intermolecular interactions in the crystal structure (Table 3). The

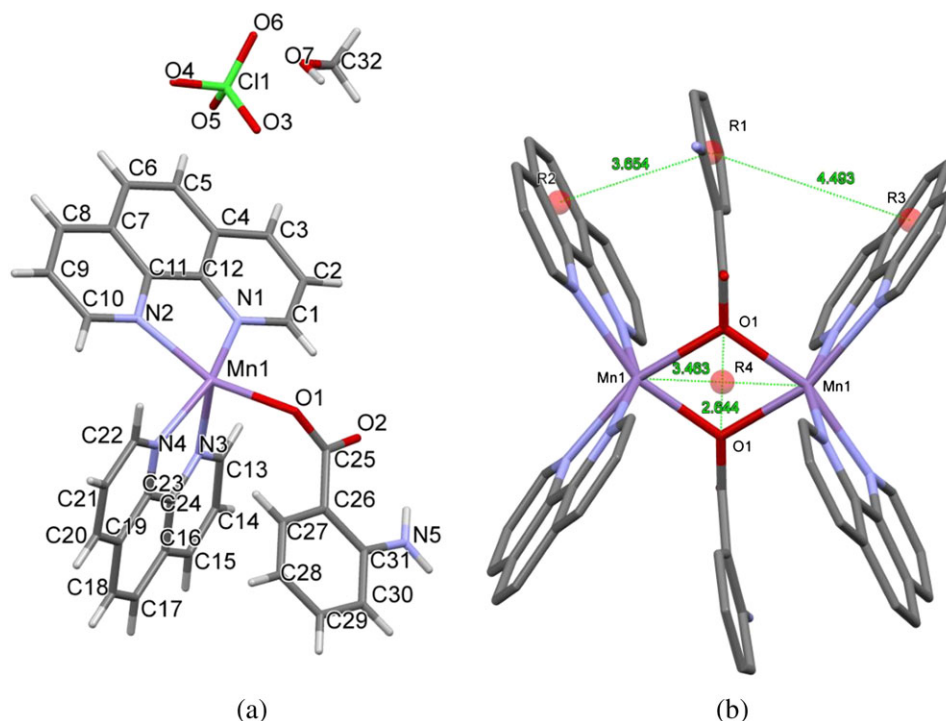


FIGURE 1 a) Asymmetric molecular structure of $[\text{Mn}_2(\mu_{1,1}\text{-}2\text{-NH}_2\text{C}_6\text{H}_4\text{COO})_2(\text{phen})_4](\text{ClO}_4)_2(\text{CH}_3\text{OH})$ (**1**) with the atom numbering scheme and b) $\pi\cdots\pi$ interaction and some atom distance in the structure

TABLE 2 Comparison of selected structural data for Mn(II) compounds with monodentate bridging mode, $[\text{Mn}_2(\mu_{1,1}\text{-O})_2]$

Compound	Mn \cdots Mn (Å)	Mn-O-Mn ($^\circ$)	Ref.
$[\text{Mn}_2(\text{dmb})_4(\text{bpy})_2(\text{H}_2\text{O})_2]\text{bpy}$	3.532	104.2	25 g
$[\text{Mn}_2(2,6\text{-dmb})_4(\text{Me}_2\text{Phen})_2(\text{H}_2\text{O})_2]2\text{EtOH}$	3.590	105.1	25f
$[\{\text{Mn}(\text{phen})_2\}_2(1\text{-}3\text{-ClC}_6\text{H}_4\text{COO})_2](\text{ClO}_4)_2$	3.469	104.9	25a
$[\{\text{Mn}(\text{phen})_2\}_2(1\text{-}3\text{-CH}_3\text{C}_6\text{H}_4\text{COO})_2](\text{ClO}_4)_2$	3.454	104.6	
$[\{\text{Mn}(\text{phen})_2\}_2(1\text{-}4\text{-ClC}_6\text{H}_4\text{-COO})_2](\text{ClO}_4)_2$	3.415	102.5	
$[\{\text{Mn}(\text{phen})_2\}_2(1\text{-}4\text{-CH}_3\text{C}_6\text{H}_4\text{COO})_2](\text{ClO}_4)_2$	3.460	103.7	
$[\text{Mn}^{\text{II}}_2(\text{bpmapa})_2(\text{H}_2\text{O})_2](\text{ClO}_4)_2$	3.688	107.6	25 h
$[\text{Mn}^{\text{II}}_2(\text{pbpmapa})_2(\text{H}_2\text{O})_2](\text{ClO}_4)_2$	3.692	107.9	
$[(\text{ac})\text{Mn}(\text{bbml})_2 \text{Mn}(\text{ac})](\text{BF}_4)3.5\text{HO}$	3.177	105.3	25i
$[\text{Mn}_2(\mu_{1,1}\text{-}2\text{-NH}_2\text{C}_6\text{H}_4\text{COO})_2(\text{phen})_4](\text{ClO}_4)_2(\text{CH}_3\text{OH})$	3.463	105.3	This work

dmb = 2,6-dimethoxybenzoato(1-), bpy = 2,2'-bipyridine, 2,6-dmb = 2,6-dimethoxybenzoate(1-), Me₂phen = 4,7-dimethyl-1,10-phenanthroline, Hbbml = [bis(2-benzimidazolylmethyl)amino]-ethanol, Hac = acetic acid, bpmapa = [bis(2-pyridylmethyl)amino]propionic acid, pbpmapa = a-phenyl-b-[bis(2-pyridylmethyl)amino]propionic acid.

binuclear complex units interact through hydrogen bonds between the uncoordinated perchlorate anions and nitrogen atom of NH₂ group of anthranilate, leading to 2D chains (Figures 3 and 4). N–HO, C–HO and C–HN type hydrogen bonds observed among the coordinated bipy, carboxylate group and free perchlorate anions. Furthermore, π - π aromatic stacking interactions between the rings of ligands stabilize the structure.

3.3 | Theoretical calculations

We examined the stability of the following structures of manganese (II) compounds $[\text{Mn}_2(\mu_{1,1}\text{-}2\text{-NH}_2\text{C}_6\text{H}_4\text{COO})_2(\text{phen})_4](\text{ClO}_4)_2(\text{CH}_3\text{OH})$ (**1**), $[\text{Mn}_2(\mu_{1,1}\text{-}2\text{-NH}_2\text{C}_6\text{H}_4\text{COO})_2(\text{phen})_4](\text{ClO}_4)_2(\text{CH}_3\text{OH})$ (**2**), $[\text{Mn}_2(\mu_{1,1}\text{-}2\text{-NH}_2\text{C}_6\text{H}_4\text{COO})_2(\text{bipy})_4]2(\text{ClO}_4)$ (**3**) and $[\text{Mn}_2(\mu_{1,3}\text{-}2\text{-NH}_2\text{C}_6\text{H}_4\text{COO})_2(\text{phen})_4]2(\text{ClO}_4)$ (**4**) using computational

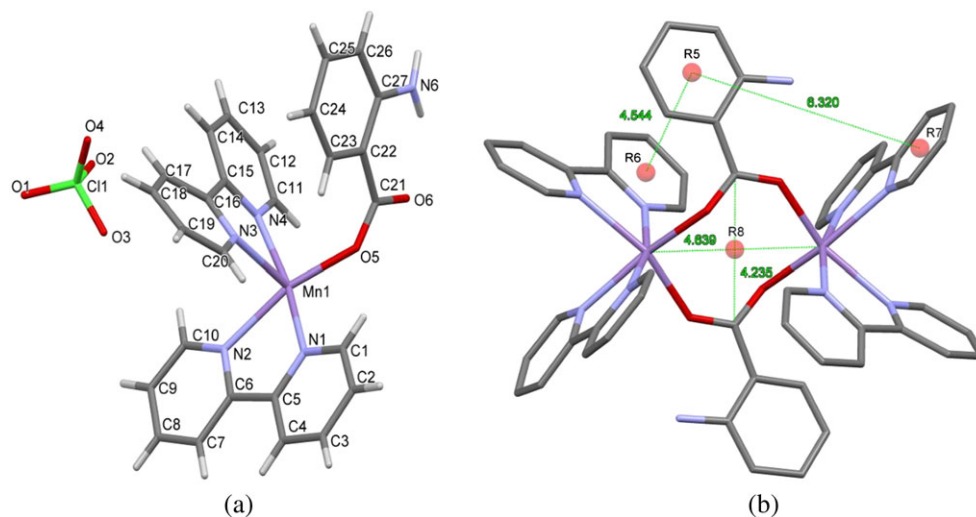


FIGURE 2 a) Asymmetric molecular structure of $[\text{Mn}_2(\mu_{1,3}\text{-}2\text{-NH}_2\text{C}_6\text{H}_4\text{COO})_2(\text{bipy})_4](\text{ClO}_4)_2$ (**2**) with the atom numbering scheme and b) $\pi\cdots\pi$ interaction and some atom distance in the structure

TABLE 3 Hydrogen bonding in compound **1** and **2**

D – H \cdots A	D – H (Å)	H \cdots A (Å)	D \cdots A (Å)	D – H \cdots A (°)
1				
N5 – H6B \cdots O2	0.86	2.06	2.696(5)	130
C1 – H1 \cdots O2	0.93	2.53	3.417(4)	160
C22 – H22 \cdots O2	0.93	2.57	3.460(3)	162
C27 – H27 \cdots O1	0.93	2.45	2.779(3)	101
C3 – H3 \cdots O3 ⁱ	0.93	2.50	3.354(7)	153
C32 – H11A \cdots N5 ⁱⁱ	0.96	2.06	3.016(8)	174
C32 – H11C \cdots O3 ⁱⁱ	0.96	2.20	2.992(10)	139
C32 – H111C \cdots O6 ⁱⁱ	0.96	2.29	3.211(10)	160
C15 – H15 \cdots O4 ⁱⁱⁱ	0.93	2.53	3.450(5)	169
C21 – H21 \cdots O2 ^{iv}	0.93	2.49	3.400(4)	162
2				
N6 – H6A \cdots O6	0.83	2.07(3)	2.687(2)	131(3)
C11 – H11 \cdots O5	0.93	2.34	3.209(2)	155
N6 – H6B \cdots O2 ^v	0.87	2.24(3)	3.076(2)	162(3)
C7 – H7 \cdots O4 ^{vi}	0.93	2.55	3.219(3)	129
C8 – H8 \cdots O6 ^{vii}	0.93	2.52	3.076(3)	119
C17 – H17 \cdots O5 ^{id}	0.93	2.46(2)	3.260(3)	144

Symmetry codes: (i) 1-x,1-y,1-z; (ii) -1 + x,y,z; (iii) 1-x,1-y,-z; (iv) -1 + x,y,z; (v) 1/2-x,3/2-y,1-z (vi) x,-1 + y,z; (vii) -x,1-y,-z

methods. **1** and **2** are crystallographically characterized, and the other two are created just for comparison purposes. The optimized geometry of the structures was given in SP3. As shown in Table 4 interestingly, the monodentate bridged compound **1** which has higher energy (18.49 kcal/mol) than optimized bidentate bridged

compound **4**, was experimentally isolated. We obtained **1** instead of **4** which is calculated theoretically more stable. It is not easy to give a clear explanation of this behavior of formation, probably some kinetic or other factors that cause the formation of the higher energy level of **1**. However, the DFT calculation on B3LYP/6-31G(d,p)

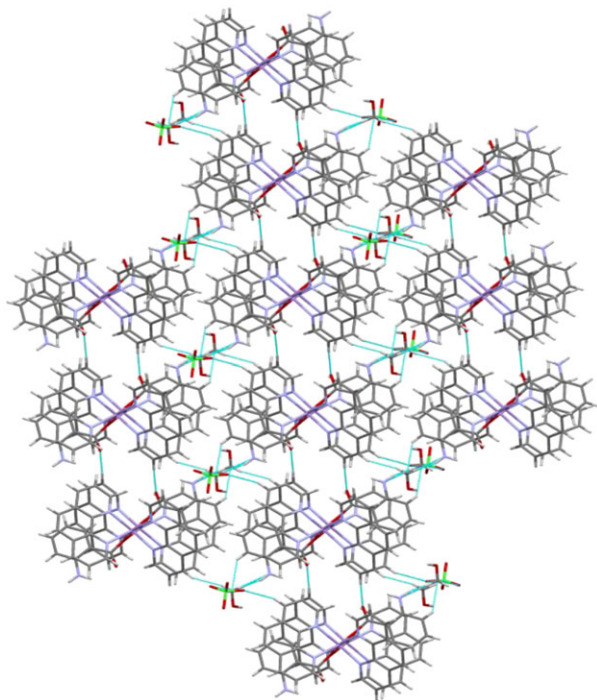


FIGURE 3 Packing arrangement of molecules of **1** in the unit cell (a long *b* axis)

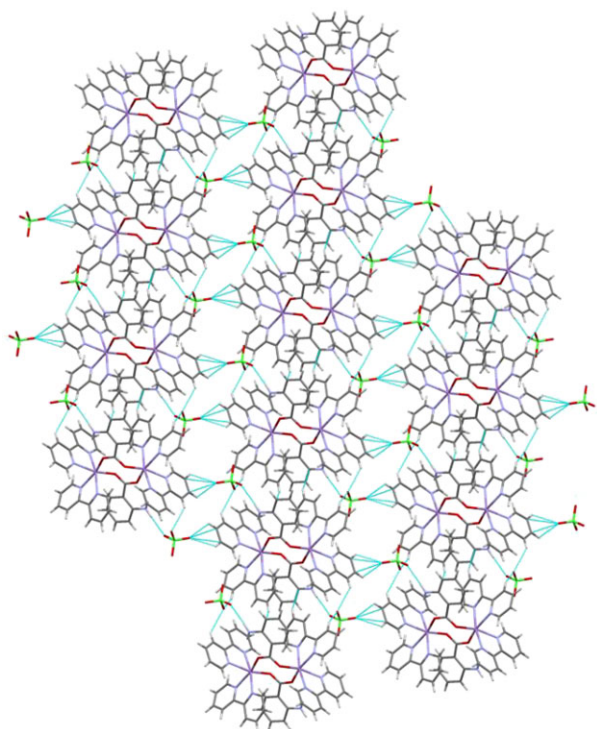


FIGURE 4 Packing arrangement of molecules of **2** in the unit cell (*b* axis)

optimized geometry showed that bidentate $\mu(1,3)$ *syn-anti* and $\mu(1,1)$ *syn-syn* bridged compound **2** has 32.16 and 31.89 Kcal/mole more energy than compound **3**. This is

TABLE 4 DFT B3LYP/6-31G(d,p)//B3LYP/6-31G(d,p)* energies and relative energies

Structure	1 (Exp.)	4 (Cal.)
Energy (in Hartree)**	- 5539.301020	-5539.330482
Relative energy (in kcal/mol)	18.49	0.00
Structure	2 (Exp.)	3 (Cal.)
Energy (in Hartree)**	-5234.397631	-5234.346811
	(<i>syn-syn</i>)	
	-5234.39806414	-5234.346811
	(<i>syn-anti</i>)	
Relative energy (in kcal/mol)	0.00	31.89 (<i>syn-syn</i>)
	0.00	32.16 (<i>syn-anti</i>)

*All calculations were carried out by 64-bit Gaussian 09 software implemented on Linux OpenMandriva.

**1Hartree = 627.50956 Kcal/mole.

the result we expected. The calculated structure **2** is fully in accordance with the experimental finding.

The previously published results of analogue compounds two factor effecting the bridging mode of carboxylate group: the steric and electronic effect of R group on phenyl ring. In our case, both effect were eliminated by using same ligand (2-amino benzoic acid) in **1** and **2**. Under similar reaction conditions, the analogue compound **2** with the use of NN type bipy ligand instead of phen ligand shows a $\mu(1,3)$ coordination mode, so the NN type ligand also seems to play an important role in different behavior observed. This result consistent with the Gomez group^[25a, b, c] published analogue Mn(II) compounds.

While in the crystal structure **1**, which is bridged with one oxygen atom of carboxylate group, the Mn^{III}-Mn distance was found to be 3.461 Å, and the same distance has been calculated as 3.318 Å. In the case of **2**, which is bridged with two oxygen atoms of carboxylate group, the crystallographically observed interaction distance between Mn(II) centers was 4.639 Å, and the calculated distance was 4.710 Å, which is very close to the experimental value. Furthermore, the calculated bond distances and angles are good agreement with an experimental values (SP4). The calculated UV and IR spectrum are also perfectly match with the experimental value (SP5 and SP6, respectively).

3.4 | Catalase-like activity

The disproportionation reaction of H₂O₂ to H₂O and O₂ (catalase activity) was studied with crystals of homobinuclear Mn(II) compounds **1** and **2**, and then the results were compared. It is worth emphasizing that the catalase activity was studied in acetonitrile (5 ml) with

the compound (3.88×10^{-6} mol and 9.7×10^{-3} mol of H_2O_2). The H_2O_2 / cat. ratio was kept constant for all experiments. The same procedure was repeated with all compounds in different solvents and Tris-HCl buffer as solvent. Blank experiments that were performed without the catalyst showed a negligible decomposition of H_2O_2 . The catalytic activity of $\text{Mn}(\text{ClO}_4)_2$ toward H_2O_2 disproportionation was tested under the same conditions as those used for the synthesis 1 and 2, $\sim 1\%$ of the H_2O_2 decomposition was observed. The same procedure was repeated with two compounds using different solvents. H_2O_2 rapidly decomposed in the presence of catalytic amounts of 1 or 2 at room temperature.

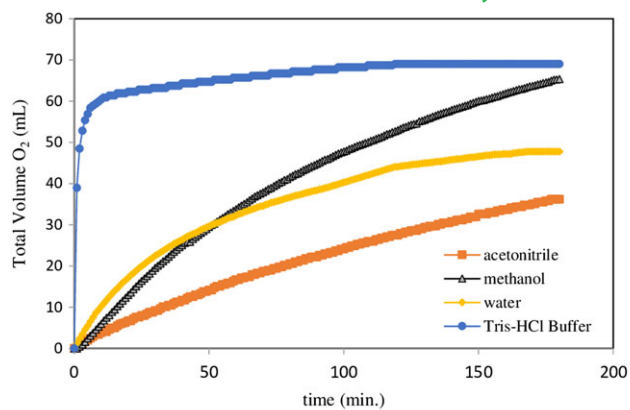
3.5 | Solvent effect

In order to find a better solvent for disproportionation of H_2O_2 by 1 and 2, acetonitrile, methanol, water and 0.1 M Tris-HCl buffer solution (pH = 7.8) were assayed, and all experiments were carried out at 25 °C (Table 5, Figure 5). In a typical experiment, the solution of compound (in 5 ml solvent) was closed in a flask with a rubber septum. After 10 min. Stirring to get a stable temperature, 1 ml (9.7×10^{-3} mol) H_2O_2 solution (30%) was injected and the volume of evolved dioxygen was measured at time intervals of 1 min. Observed initial rates were expressed as ml s^{-1} by taking the volume of the evolved oxygen into account and calculated from the maximum slope of curve describing evolution of O_2 versus time graph (Table 5, Figure 5). It was found that the initial rates are strongly dependent on the solvent. Induction period was not observed in any of the studied solvents. As shown in Table 5, when the initial rates are compared, compound 1 appears to be the more effective catalyst, except in the Tris-HCl buffer solution. Significantly, the activity of 1 is relatively low compared to 2, which is surprising, since the Mn-Mn distance (3.463 \AA in 1) is smaller than that

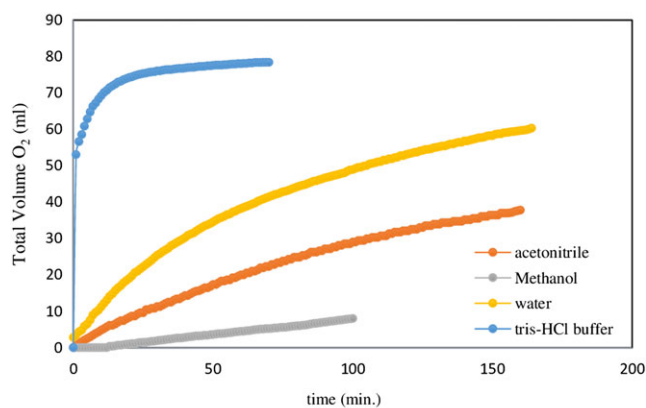
TABLE 5 H_2O_2 disproportionation with 1–2 in different solvents

Complex	Solvent	Total O_2 (mL)	$v_i \times 10^{-2}$ (mL s^{-1})	TOF (h^{-1})
1	Acetonitrile	36	0.64	243
	Methanol	48	1.08	414
	Water	65	1.72	656
	Tris-HCl Buffer	69	50.0	12640
2	Methanol	10	0.13	51
	Acetonitrile	38	0.67	263
	Water	58	1.45	552
	Tris-HCl Buffer	78	100.0	17910

Reaction conditions: $T = 25$ °C, $\text{H}_2\text{O}_2 = 9.7 \times 10^{-3}$ mol (1 ml) (1.62 M), catalyst = 3.88×10^{-6} mol (6.47×10^{-4} M) solvent = 5 ml. Initial rates defined as $V(\text{O}_2)/t$



(a)



(b)

FIGURE 5 Disproportionation reaction with 1 a) and 2 b) in different solvents

found in the manganese-catalase from *Thermus thermophilus* (3.60 \AA).^[4]

When the reaction was carried out at 25 °C in Tris-HCl buffer solution, which corresponds to the physiological conditions of the cell environment, the catalase activity of complexes showed dramatic improvement of oxygen evolution rate of $50 \times 10^{-2} \text{ mL s}^{-1}$ (66% disproportionation) with 1 and $100 \times 10^{-2} \text{ mL s}^{-1}$ (58% disproportionation) with 2. Thus, the results suggest that both complexes would also be an active catalyst in vitro. The rate of decomposition is almost 29 times and 45 times faster in Tris-HCl buffer than in water solution for 1 and 2, respectively.

The most active decomposition is obtained in Tris-HCl buffer for both compounds (TOF = 12640 h^{-1} for 1, and TOF = 17910 h^{-1} for 2) (Table 5 and Figure 5). We could not observe the systematic correlation between the activity of 1 with the relative dielectric constants of solvents, whereas the activity of 2 increases in the order of the relative dielectric constants: Tris-HCl buffer (TOF = 17910 h^{-1} , $v_i = 100 \times 10^{-2} \text{ mL s}^{-1}$) > water (TOF = 552 h^{-1} , $v_i = 1.45 \times 10^{-2} \text{ mL s}^{-1}$) > acetonitrile (TOF = 263 h^{-1} , $v_i = 0.67 \times 10^{-2} \text{ mL s}^{-1}$) > methanol

TABLE 6 Base effect on catalase activity of compounds **1**–**2** in water

Complex	Additive	Add./cat.	Total O ₂ (ml)	$v_i \times 10^{-2}$ (ml s ⁻¹)	TOF (h ⁻¹)
1	Without	-	65	1.72	656
	NaOH	1:1	44	1.85	865
		3:1	43	7.14	2717
		5:1	54	41.7	15840
	Imidazole	1:1	46	2.17	827
		3:1	55	3.03	1189
		5:1	54	4.76	1585
2	Without	-	58	1.45	532
	NaOH	1:1	94	4.76	1806
		3:1	108	16.7	6324
		5:1	113	62.3	23600
		Imidazole	1:1	71	2.70
	3:1	98	3.03	1189	
	5:1	125	4.76	1869	

Reaction conditions: $T = 25\text{ }^\circ\text{C}$, $\text{H}_2\text{O}_2 = 9.7 \times 10^{-3}$ mol (1 ml), catalyst = 3.88×10^{-6} mol, solvent = 5 ml water.

(TOF = 51 h^{-1} , $v_i = 0.13 \times 10^{-2}$ mL s⁻¹). The observed activity in different solvents indicates that Mn(II)-solvent coordination is essential to the catalytic cycle.

3.6 | Base effect

The addition of some organic and inorganic base during catalytic reaction has previously been shown to improve the catalase activity.^[26] It was suggested that the base deprotonates the H_2O_2 to initiate the catalytic reaction via binding to active center of catalyst. In contrast to those reported Mn(II) compounds, **1** and **2** exhibited catalase activity without addition of base (SP7 and SP8). Despite this, to further understand H_2O_2 decomposition by binuclear Mn-carboxylate **1** and **2**, we investigated the effect of strong inorganic base (NaOH) and weak heterocyclic organic base (imidazole) which are known to exist in the vicinity of the active sites of the manganese enzymes. Base in different mole ratios of catalyst (catalyst/base, 1:1, 1:3 and 1:5) was added to the flask before H_2O_2 was introduced. Experiments were carried out in water at $25\text{ }^\circ\text{C}$. Lag phase was not observed for the reaction with or without addition of NaOH. In Table 6 (SP7 and SP8), the turnover numbers for the disproportionation of H_2O_2 by the manganese compounds in the absence and presence of different amounts of base are compared. Our observations showed that the addition of both type of base enhanced the activity of compounds. Similar to related

TABLE 7 Oxidation of alkenes with **1**

Time (min.)	Cyclohexene	Styrene	Ethyl benzene	1-octene	1-hexene
	Tot. conv. (%) ^f	Tot. conv. (%)	Tot. conv. (%)	Tot. conv. (%)	Tot. conv. (%)
0	0	0	0	0	0
1	36.2	0	3.9	0.4	13.6
15	73.4	8.7	6.1	2.9	36.4
30	82.9	19.3	9.0	4.9	46.5
45	87.4	21.9	11.3	5.9	56.8
60	91.5	26.7	22.6	9.7	66.0
90	95.2	27.3	36.8	26.6	77.8
120	97.3	30.3	37.5	43.2	78.7
150	98.1	31.7	38.9	55.0	81.3
180	98.8 ^a	32.6	41.4	57.3	82.9
240		35.8	43.3	71.0	84.6
300		38.5	49.1	86.7	88.2
360		38.7	53.0	92.7	100 ^e
1440		51.2 ^b	79.4 ^c	98.0 ^d	

^aAfter 3 h. of reaction: product distribution 4.5% cyclohexene oxide, 85.1% cyclohexene-1-on, 9.2% 1,2-hexenediol.

^bAfter 24 h. of reaction: product distribution 2.9% benzaldehyde, 1.8% styrene oxide, 39.1% acetophenone, 7.4% 2-phenyl ethanol.

^cProduct distribution acetophenone one product.

^dAfter 24 h. of reaction: product distribution one product hexenoic acid.

^eAfter 6 h. of reaction: product distribution 24.9% 1-hexene-1-one, 51% hexanal, 24.1% 2,5 hexenedione.

^fThe yields were determined by using GC.

Conditions: 1.45×10^{-2} mole of TBHP, subs./cat.(in mol) = 265, $70\text{ }^\circ\text{C}$, solvent = acetonitrile.

published studies, the initial reaction rates of our catalytic system increased with increasing base concentration. Interestingly, the base enhancement was not stoichiometrically proportional to the base concentration, which probably suggests that they may not only coordinate to manganese. In contrast to imidazole addition, addition of NaOH causes a significant enhancement of the rate. The dramatic improvement of activity with addition of three equivalent NaOH was obtained for both compounds, and the initial rates increased ~ 24 times ($1.72 \times 10^{-2} \text{ ml s}^{-1}$ (TOF = 656 h^{-1}) to $41.7 \times 10^{-2} \text{ ml s}^{-1}$ (TOF = 15840 h^{-1}) for **1** and ~ 43 times ($1.45 \times \text{ml s}^{-1}$ (TOF = 532 h^{-1}) to $62.3 \times 10^{-2} \text{ ml s}^{-1}$ (TOF = 23600 h^{-1}) for **2** compared to without base. On the contrary, the addition of imidazole less effective than strong base (Table 6). The initial rates increased ~ 3 times with addition of three equivalent imidazole for both compounds.

Nonetheless, published results showed that the catalase activity only occurred between MnII,II to MnIII, III, and higher oxidation states than MnIII are catalytically inactive.^[27] Thus the activities of manganese ion containing compounds with different oxidation states and different numbers of carboxylate ligands and also in different bridging coordination modes (i.e. $\mu_{1,1}$ and $\mu_{1,3}$) are not comparable. There are other manganese compounds having carboxylate ligands that have been

reported, but the correlations between manganese compounds' activity and the coordination modes of their bridging carboxylate ligands, the ligand type and the number, etc. are not fully understood.^[28] The catalase activities of analogous $\mu_{1,3}$ -RCOO bridged binuclear Mn(III) compounds with other substituents on the benzoate ligands have been reported under similar experimental conditions.^[9,25c] For compounds with bidentate bridging mode, in our case Mn(II) compounds with bidentate carboxylate bridged have a quite good correlation between the catalase activity. Only one reported catalase activity result was found for compound which has monodentate bridged.^[25h] In acetonitrile at 30°C conditions, in our case, the initial disproportionation rate ($0.64 \times 10^{-2} \text{ ml s}^{-1}$) of **1** is similar with compounds $[\text{Mn}^{\text{II}}2(\text{pbpmapa})_2(\text{H}_2\text{O})_2](\text{ClO}_4)_2$ ($0.3 \times 10^{-2} \text{ mL s}^{-1}$) and $[\text{Mn}^{\text{II}}2(\text{bpmapa})_2(\text{H}_2\text{O})_2](\text{ClO}_4)_2$ ($2.1 \times 10^{-2} \text{ ml s}^{-1}$).

3.7 | Oxidation activity

The catalytic ability of homobinuclear manganese compounds **1** and **2** in oxidation of alcohols and alkenes with TBHP has been studied in acetonitrile at 70°C . Substrate / catalyst ratio (265) was kept constant in all catalytic reactions. Turnover numbers are around 30–50, while the turnover frequencies are only moderate

TABLE 8 Oxidation of alkenes with **2**

Time (min.)	Cyclohexene	Styrene	Ethyl benzene	1-octene	1-hexene
	Tot. conv. (%)	Tot. conv. (%)	Tot. conv. (%)	Tot. conv. (%)	Tot. conv. (%)
0	0	0	0	0	0
1	15.2	0.8	0	2.4	16.1
15	66.4	3.6	5.7	6.2	20.0
30	80.4	5.4	5.9	8.9	37.5
45	85.0	5.6	14.1	12.2	45.3
60	85.4	6.8	17.1	16.8	52.4
90	92.4	7.4	23.6	35.2	85.6
120	96.2	7.6	31.0	45.9	94.3
180	98.0	9.4	38.5	62.2	100 ^e
240	98.9 ^a	10.0	41.9	75.9	
300		10.6	43.0	83.0	
360		10.7	55.2	94.2	
1440		25.2 ^b	85.7 ^c	99.0 ^d	

^aAfter 4 h. of reaction: product distribution 3.9% cyclohexene oxide, 84.1% cyclohexene-1-on, 10.9% 1,2-hexanediol

^bAfter 24 h. of reaction: product distribution 2.5% benzaldehyde, 1.0% styrene oxide, 21.3% acetophenone

^cProduct distribution acetophenone one product.

^dAfter 24 h. of reaction: product distribution one product hexenoic acid

^eAfter 3 h. of reaction: product distribution 28.9% 1-hexene-1-one, 45.4% hexanal, 25.7% 2,5 hexenedione

Conditions: 1.45×10^{-2} mole of TBHP, subs./cat.(in mol) = 265, 70°C , solvent = acetonitrile

(TOF = 2–20 h⁻¹) in the synthetic catalytic oxidation systems using H₂O₂ and TBHP. In our oxidative system, poor activity for styrene (TOF = 8 h⁻¹ with **2**), moderate activity for styrene, ethyl benzene and 1-octene (TOF = 34–51 h⁻¹) and good activity for cyclohexene and 1-hexene were obtained for both compounds (TOF = 152–302 h⁻¹).

3.8 | Oxidation of alkenes

The catalytic oxidation of cyclohexene, styrene, 1-hexene, 1-octene and ethyl benzene exhibit good activity without adding any additives. The Mn(II)/TBHP/olefin/CH₃CN system showed higher activity with electron-rich alkenes (i.e. cyclohexene) and relatively low activity with electron-deficient alkenes (i.e. ethyl benzene and styrene)

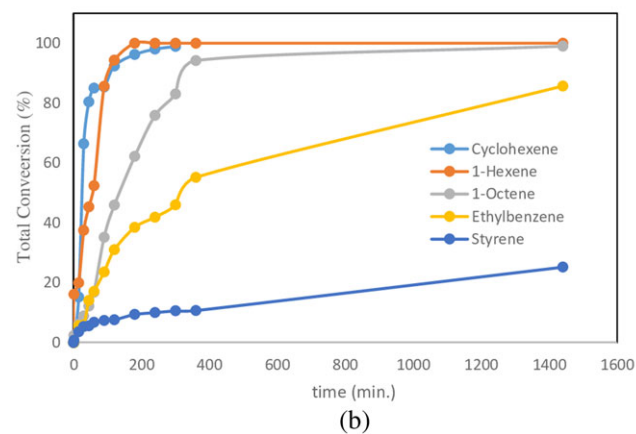
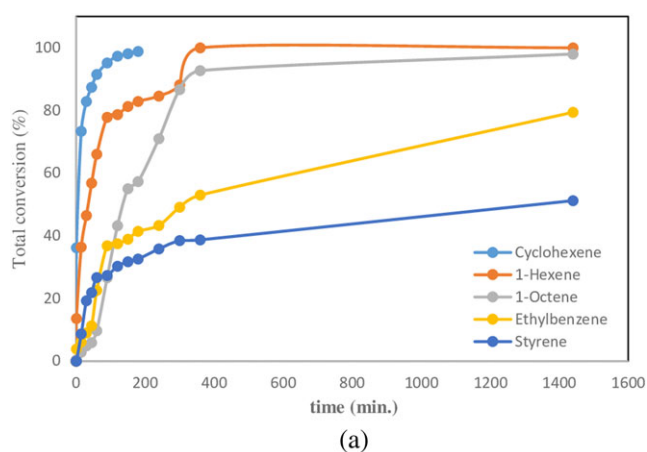


FIGURE 6 Alkene oxidation with compounds **1** (a) and **2** (b)

under similar reaction conditions. The experimental results that are shown in Tables 7, 8 and Figure 6 represent the maximum total conversions and depend on the time for oxidation using TBHP as an oxidant in at 70 °C in CH₃CN.

Compounds **1** (98.8%, after 3 h.) and **2** (98.9% after 4 h.) showed the highest activity of cyclohexene oxidation to cyclohexanone (yields 84.1% and 85.1% with **1** and **2**, respectively) with the small amounts of 1,2-hexendiol and cyclohexene oxide. Cyclohexene has two fragments that are accessible to attack by the catalytically active species (the double bond and relatively weak C–H bonds).

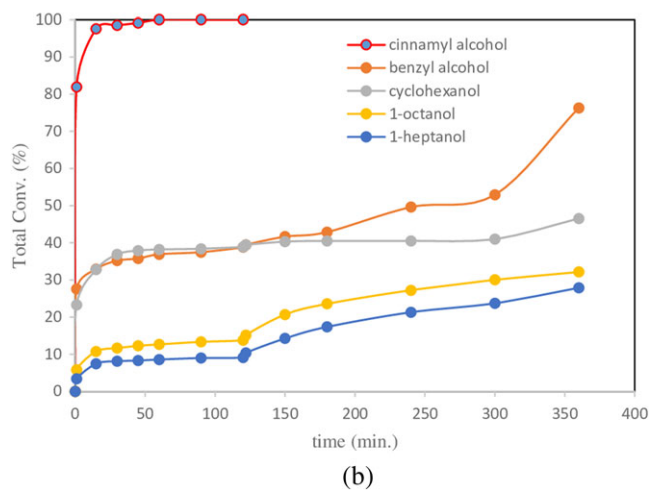
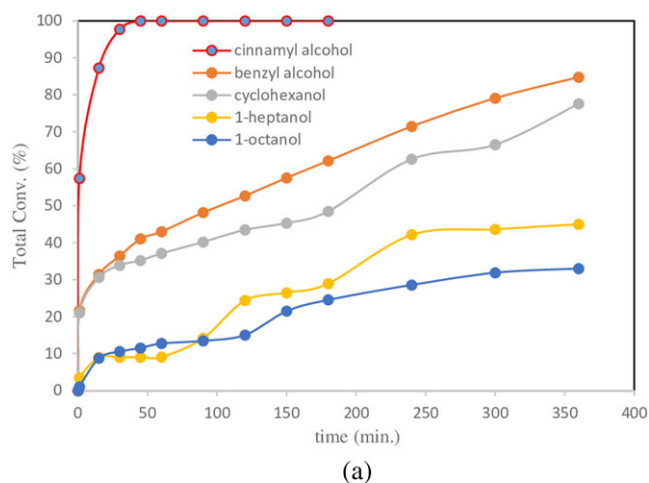


FIGURE 7 Alcohol oxidation with compounds **1** (a) and **2** (b)

TABLE 9 Catalytic activity comparison of compounds **1** and **2** for alkene oxidation in 1 hour reaction

Complex	Cyclohexene		Styrene		Ethyl benzene		1-octene		1-hexene	
	TON	TOF (h ⁻¹)	TON	TOF (h ⁻¹)	TON	TOF (h ⁻¹)	TON	TOF (h ⁻¹)	TON	TOF (h ⁻¹)
1	243	243	80	40	100	50	230	46	207	138
2	226	226	25	8	102	34	202	51	227	152

TON = turnover number (mol of substrate/mol of catalyst)

Comparison of the rates of epoxidation and C–H bond oxygenation could give valuable information on the nature of the oxidizing species. In our catalytic system, the absence of the epoxidation product indicates that the reaction proceeded mainly through C–H bond activation. The allylic ketone formation strongly shows that the catalytic oxidation undergoes by radical oxidant.^[9] Compound **1** oxidized mainly cyclohexene to cyclohexanone (76%), and other products – 2-cyclohexen-1-ol (2.6%), cyclohexene oxide (4.5%) and 1,2-cyclohexendiol (8.4%) – and TON is 243 within 1 h (TOF = 243 h⁻¹) based on the total yield of products (total conv. 91.5% in 1 h., Tables 5 and 7). Compound **2** exhibits very fast oxidation reaction under the similar conditions (100% conversion in 1 h with 85.4% conversion: 2-cyclohexen-1-one (69.6%), cyclohexene oxide (4.7%), 2-cyclohexen-1-ol (2.8%) and 1,2-cyclohexendiol (8.3%), and the TON is 226 within 1 h (TOF = 226 h⁻¹) based on the total products (Tables 7, 8).

Very low catalytic activity was observed for oxidation of electron deficient styrene with **1** and **2**. The major final product is acetophenone (85% selectivity, 51.1% yield with **1** and 76% selectivity, 25.2% yield with **2**) after 24 h

reaction (Tables 7, 8). Styrene oxidation shows the slowest kinetic profile among the other olefins (Figure 6).

The oxidation of ethyl benzene to acetophenone with excellent selectivity exhibited a high conversion for both compounds (~100% conversion) with TBHP in acetonitrile at 70 °C. In contrast to reported Mn(II) compounds, remarkable results have been obtained for terminal olefins 1-hexene, and 1-octene gave ~100% conversion for both catalysts. Although 1-hexene, which is a rather hard oxidation substrate, **1** and **2** exhibited very high activity for the oxidation of 1-hexene, affording 51% and 45.4% hexanal, for **1** and **2**, respectively, as a major product with the formation of other products, 24.9%; 28.9% 1-hexene-1-one and 24.1%; 25.7% 2,5 hexenedione for **1** and **2**, respectively. The TOF value of **1** is 138 h⁻¹ (after 6 h) and 152 h⁻¹ (after 3 h) for **2** (Table 9).

In comparison to other similar Mn(II) compounds, **1** and **2** are generally superior, according to their higher conversion and selectivity.^[29] For example, in our previous work,^[10a] when a binuclear Mn(II) compound, [Mn₂(μ_{1,3}-C₆H₅COO)₂(bipy)₄](ClO₄)₂, in acetonitrile with TBHP as oxidant in 70 °C, by the same stoichiometric amounts as this paper, after 4 h. reaction, while the

TABLE 10 Oxidation of alcohols with **1**

Time (min.)	Cinnamyl alcohol	Benzyl alcohol	Cyclohexanol	1-octanol	1-heptanol
	Tot. conv. (%)	Tot. conv. (%)	Tot. conv. (%)	Tot. conv. (%)	Tot. conv. (%)
0	0	0	0	0	0
1	57.4 ^a	21.6	26.8	1.03	3.5
15	87.3	31.4	37.7	8.8	8.9
30	97.8	36.4	41.5	10.6	9.0
45	100.0 ^b	41.1	42.5	11.5	9.1
60		43.0 ^c	44.9	12.8	9.1
90		48.2	47.9	13.5	9.2
120		52.7	51.1	15.0	26.4
150		57.5	53.3	21.5	26.5
180		62.2	55.8	24.5	27.0
240		71.5	71.7	28.6	43.2
300		79.1	75.7	31.9	43.6
360		84.8	77.6	33.0 ^f	44.9
1440		100.0 ^d	88.2 ^e	46.6	67.2 ^g

^aAfter 1 min. of reaction: product distribution 13.9% benzaldehyde, 43.5% cinnamaldehyde.

^bAfter 45 min. of reaction: product distribution 15.8% styrene, 41.6% benzaldehyde, 20.4% cinnamaldehyde, 22.3% 3-phenyl glycidole.

^cAfter 1 h. of reaction: product distribution 40.0% benzaldehyde, 3.0% benzoic acid.

^dAfter 24 h. of reaction: product distribution 100% benzoic acid.

^eAfter 24 h. of reaction: product distribution selectivity 100% cyclohexanone.

^fAfter 6 h. of reaction: product distribution 24.7% heptaldehyde, 4.9% heptanoic acid, 2.0% octanoic acid.

^gAfter 24 h. of reaction: product distribution selectivity 100% heptaldehyde.

Conditions: 1.45 × 10⁻² mole of TBHP, subs./cat.(in mol) = 265, 70 °C, solvent = acetonitrile.

conversion of 94.3% in the oxidation of cyclohexene, the conversion of ~100% was obtained with **1** and **2** after 1.5 h. The good catalytic activity was obtained for oxidation of ethyl benzene with **1** (79.4%) and **2** (85.7%) than in our previous work (11.0%) in total conversion after 24 h reaction.

3.9 | Oxidation of alcohols

Compounds **1** and **2** exhibited high activity for the oxidation of primary alcohols, cinnamyl, benzyl alcohol and cyclohexanol and low activity for 1-octanol and 1-heptanol. The time-dependent catalytic activity results are compared in Figure 7 and Tables 10 and 11. Among the studied alcohols, cinnamyl alcohol is the most active one and resulted in ~100% conversion in 45 min. (TON ~266) with both compounds. It should be noted that the catalytic rate of cinnamyl alcohol oxidation is extremely high: TOF = 13040 h⁻¹ and 9180 h⁻¹ in first minute of the reaction, respectively with **1** and **2**. Primary aliphatic alcohols were oxidized to carboxylic acids as

their secondary oxidation products, whereas secondary alcohol (cyclohexanol) were oxidized to the cyclohexanone (77.6% with **1** and 45.8% with **2** in acetonitrile, 6 h) without carbon-carbon chain cleavage. These results supports the reports that benzylic alcohols are more reactive than aliphatic alcohols.^[26]

Primary aliphatic alcohol, 1-octanol, was oxidized to heptaldehyde and its carboxylic acid in a moderate conversion of 33.0% with **1** and 32.1% with **2** in 6 h. reaction.; heptaldehyde (24.7%), heptanoic acid (4.9%) and octanoic acid (2.0%) with **1** and heptaldehyde (24.9%) and heptanoic acid (6.1%) with **2** (Table 10, for **1**). Benzyl alcohol converted to the benzaldehyde and benzoic acid (total conv., 100% and 76.3% in 24 h with **1** and **2**, respectively) (Tables 10, 11). In the first 1.5 h of reaction, the maximum aldehyde conversion was obtained (45.3%) with 79% aldehyde selectivity; further, the reaction proceeds, and the over oxidation observed in 100% benzoic acid formed in 24 h reaction with **1**. Whereas for **2**, during the same time intervals, 39.4% aldehyde formation was observed as one product in 1.5 h and after a 24 h reaction, the product distribution is 39.5% aldehyde and 36.8%

TABLE 11 Oxidation of alcohols with **2**

Time (min.)	Cinnamyl alcohol	Benzyl alcohol	Cyclohexanol	1-octanol	1-heptanol
	Tot. conv. (%)				
0	0	0	0	0	0
1	81.9 ^a	27.6	25.9	5.8	3.5
15	97.6	32.9	37.3	10.8	8.8
30	98.5	35.2	41.8	11.7	9.0
45	99.2 ^b	35.8	42.9	12.3	9.1
60	100.0	36.9 ^c	43.2	12.7	9.1
90		37.5	43.2	13.3	14.2
120		38.8	43.4	13.8	24.4
150		39.4	44.3	20.7	26.4
180		41.6	44.4	23.9	17.4
240		48.9	45.0	27.2	28.9
300		49.6	45.1	30.0	23.7
360		52.9	45.8	32.1 ^f	27.9 ^g
1440		76.3 ^d	50.7 ^e	47.6	35.5 ^g

^aAfter 1 min. of reaction: product distribution 2.9% styrene, 27.4% benzaldehyde, 48.9% cinnamaldehyde, 2.7% 3-phenyl glycidole.

^bAfter 45 min. of reaction: product distribution 18.9% styrene, 40.1% benzaldehyde, 25.4% cinnamaldehyde, 8.1% 3-phenyl glycidole, 2.2 3-phenyl-1-propanol, 1.9% cinnamic acid.

^cAfter 1 h. of reaction: product distribution 43.2% benzaldehyde (selectivity 100%).

^dAfter 24 h. of reaction: product distribution 39.5% benzaldehyde, 36.8% benzoic acid.

^eAfter 24 h. of reaction: product distribution selectivity 100% cyclohexanone.

^fAfter 6 h. of reaction: product distribution 24.9% heptaldehyde, 6.1% heptanoic acid.

^gAfter 6 h and 24 h. of reaction: product distribution selectivity 100% heptaldehyde.

Conditions: 1.45 × 10⁻² mole of TBHP, subs./cat.(in mol) = 265, 70 °C, solvent = acetonitrile.

TABLE 12 Catalytic activity comparison of **1** and **2** for alcohol oxidation

Complex	Cinnamyl alcohol		Benzyl alcohol		Cyclohexanol		1-octanol		1-heptanol	
	TON	TOF (h ⁻¹)	TON	TOF (h ⁻¹)	TON	TOF (h ⁻¹)	TON	TOF (h ⁻¹)	TON	TOF (h ⁻¹)
1	153 ^a	9180	58	3480	71	4260	3	180	9	540
	232 ^b	928	84	336	100	400	23	92	24	96
2	217 ^a	13040	73	4380	69	4140	15	900	9	542
	259 ^b	1036	87	348	99	396	29	116	20	80

^aReaction time 1 min.^bReaction time 15 min.

benzoic acid. 1-heptanol was oxidized also in moderate yield with only one product of heptaldehyde (32.1% for **1** and 27.9% for **2** in 6 h) (Tables 10, 11). It should be noted that the initial catalytic rate of benzyl alcohol (TOF = 3480 h⁻¹ with **1**, TOF = 4380 h⁻¹ with **2**) and cyclohexanol (TOF = 4260 h⁻¹ for **1**, TOF = 4140 h⁻¹ for **2**) is very high for both compounds (Table 12). In comparison of our previous work, we obtained that the previous work has better catalytic activity in oxidation of benzyl alcohol, cyclohexanol 1-octanol and 1-heptanol.^[10a]

4 | CONCLUSION

Two homobinuclear Mn(II) compounds with different carboxylate-Mn coordination modes (mono- and bidentate), [Mn₂(μ_{1,1}-2-NH₂C₆H₄COO)₂(phen)₄](ClO₄)₂(CH₃OH) (**1**) and [Mn₂(μ_{1,3}-2-NH₂C₆H₄COO)₂(bipy)₄](ClO₄)₂ (**2**), which are mimic to the catalase enzyme, were synthesized, characterized and shown to be catalase-like, and their catalytic properties were investigated for various alcohols and alkenes. The theoretical calculations showed that bidentate coordination mode has lower energy than monodentate coordination. We found that the compound with a bidentate bridging carboxylate ligand exhibits higher catalase-like activity than compounds with monodentate carboxylate ligands. Both complexes exhibited remarkable activity (TOF up to 12640 h⁻¹ with **1**, and 17910 h⁻¹ with **2**) in Tris-HCl buffer at room temperature. Moreover, we have also found that, besides TOF, the rate of the reaction dramatically increase with the addition of base (NaOH) whereas the increase in imidazole addition is weak.

We determined that in terms of the comparison of catalytic efficiency of mono- and bidentate-bridging modes, binuclear Mn(II) compounds **1** and **2** are quite close to each other in studied alcohol and alkene oxidation. The compounds exhibited very high catalytic activity in the oxidation of cinnamyl alcohol and moderate activity in benzyl alcohol and cyclohexanol and poor activity in linear alcohol 1-octanol and 1-hexanol when TBHP was used as an oxidant in an acetonitrile solvent.

In particular for cinnamyl alcohol, a conversion ratio 57.4% (TOF = 9180 h⁻¹) and 81.9% (13040 h⁻¹) and aldehyde selectivity up to 76% and 93% were observed in the first minute of reaction at 70 °C in acetonitrile for **1** and **2**, respectively. The oxygen transfer activity of **1** and **2** towards various alkenes and alcohols decreases in the following order: Cyclohexene > 1-hexene > 1-octene > ethyl benzene > styrene and cinnamyl alcohol > benzyl alcohol > cyclohexanol > 1-octanol > 1-hexanol. Thus, electron-rich cyclic olefin is more active than the electron-poor terminal olefins. This reflects the electrophilic nature of oxygen transfer from manganese-oxo intermediate to the olefin double bond.

ACKNOWLEDGEMENT

This work was financially supported by The Scientific and Technological Research Council of Turkey (TUBITAK) (Grant No. 113Z303) and Anadolu University (BAP) (Grant No. 1406F390) and the authors gratefully acknowledge the Medicinal Plants and Medicine Research Centre of Anadolu University, Eskişehir, Turkey, for the use of X-ray Diffractometer. EU COST Action CM1402 “Crystalize” is acknowledged for discussion.

ORCID

Esra Su  <http://orcid.org/0000-0002-6944-3972>

Alaettin Guven  <http://orcid.org/0000-0003-3668-6852>

REFERENCES

- [1] a) H. Sies, *Angew. Chem.* **1986**, *25*, 1058; b) S. R. Doctrow, K. Huffman, C. B. Marcus, G. Tocco, E. Malfroy, C. A. Adinolfi, H. Kruk, K. Baker, N. Lazarowych, J. Mascarenhas, B. J. Malfroy, *J. Med. Chem.* **2002**, 4549.
- [2] a) C. Kunsch, R. M. Medford, *Circ. Res.* **1999**, *85*, 753; b) M. Devereux, M. McCann, D. O'Shea, M. O'Connor, E. Kiely, V. McKee, D. Naughton, A. Fisher, A. Kellett, M. Walsh, D. Egan, C. Deegan, *Bioinorg. Chem. Appl.* **2006**, *1*, 1; c) R. M. Roat-Malone, *Bioinorganic Chemistry – A Short Course*, John Wiley and Sons Inc, Hoboken, NJ **2002** 125; d) P. Chelikani, I. Fita, P. C. Loewen, *Cell. Mol. Life Sci.* **2004**, *61*, 192.

- [3] R. H. Haschke, J. M. Friehoff, *Biochem. Biophys. Res. Commun.* **1978**, 1039.
- [4] Y. Kono, I. J. Fridovich, *J. Biol. Chem.* **1983**, 258, 6015.
- [5] V. V. Barynin, P. D. Hempstead, A. A. Vagin, S. V. Antonyuk, W. R. Melik-Adamyan, V. S. Lamzin, P. M. Harrison, P. J. J. Artymyuk, *J. Inorg. Biochem.* **1997**, 67, 196.
- [6] a) S. V. Antonyuk, W. R. Melik-Adamyan, A. N. Popov, V. S. Lamzin, P. D. Hempstead, P. M. Harrison, P. J. Artymyuk, V. V. Barynin, *Crystallogr. Rep.* **2000**, 45, 105; b) V. V. Barynin, M. M. Whittaker, S. V. Antonyuk, V. S. Lamzin, P. M. Harrison, P. J. Artymyuk, J. W. Whittaker, *Structure* **2001**, 9, 725.
- [7] a) S. V. Khangulov, V. V. Barynin, N. V. Voevodskaya, A. I. Grebenko, *Biochim. Biophys. Acta* **1990**, 1020, 305; b) G. C. Dismukes, *Chem. Rev.* **1996**, 96, 2909.
- [8] a) W. Rüttinger, G. C. Dismukes, *Chem. Rev.* **1997**, 97, 1; b) A. Gelasco, S. Bensiek, V. L. Pecoraro, *Inorg. Chem.* **1998**, 37, 3301; c) P. Kar, M. G. B. Drew, A. Ghosh, *Inorg. Chim. Acta* **2013**, 405, 349; d) A. E. M. Boelrijk, G. C. Dismukes, *Inorg. Chem.* **2000**, 39, 3020; e) S. J. Brudenell, L. Spiccia, A. M. Bond, G. D. Fallon, D. C. R. Hockless, G. Lazarev, P. J. Mahon, E. R. T. Tiekink, *Inorg. Chem.* **2000**, 39, 881; f) C. Palopoli, M. Gonzalez-Sierra, G. Robles, F. Dahan, J. P. Tuchagues, S. Signorella, *J. Chem. Soc., Dalton Trans.* **2002**, 3813; g) M. Kose, V. McKee, *Polyhedron* **2014**, 75, 30; h) L. Dubois, R. Caspar, L. Jacquamet, P. E. Petit, M. F. Charlot, C. Baffert, M. N. Collomb, A. Deronzier, J. M. Latour, *Inorg. Chem.* **2003**, 42, 4817; i) D. Moreno, C. Palopoli, V. Daier, S. Shova, L. Vendier, M. G. Sierra, J. P. Tuchagues, S. Signorella, *Dalton Trans.* **2006**, 5156; j) I. Kani, C. Darak, O. Sahin, O. Buyukgungor, *Polyhedron* **2008**, 27, 1238; k) J. A. Lessa, A. Horn Jr., E. S. Bull, M. R. Rocha, M. Benassi, R. R. Catharino, M. N. Eberlin, A. Casellato, C. J. Noble, G. R. Hanson, G. Schenk, G. C. Silva, O. A. C. Antunes, C. Fernandes, *Inorg. Chem.* **2009**, 48, 4569; l) C. Palopoli, N. Bruzzo, C. Hureau, S. Ladeira, D. Murgida, S. Signorella, *Inorg. Chem.* **2011**, 50, 8973; m) G. N. Ledesma, E. Anxolabéhère-Mallart, E. Rivière, S. Mallet-Ladeira, C. Hureau, S. R. Signorella, *Inorg. Chem.* **2014**, 53, 2545; n) M. Zienkiewicz, A. Jabłońska-Wawrzycka, J. Szlachetko, Y. Kayser, K. Stadnicka, W. Sawka-Dobrowolska, J. Jezierska, B. Barszcz, J. Sá, *Dalton Trans.* **2014**, 43, 8599; o) I. Kani, Ö. Atliler, K. Güven, *J. Chem. Sci.* **2016**, 128(4), 523.
- [9] a) J. H. Espenson, T. H. Zauche, *Inorg. Chem.* **1998**, 37, 6827; b) G. Barak, J. Dakka, Y. Sasson, *J. Org. Chem.* **1988**, 53, 3553; c) S. Das, T. Punniyamurthy, *Tetrahedron Lett.* **2003**, 44, 6033; d) Z. Ye, Z. Fu, S. Zhong, F. Xie, X. Zhou, F. Liu, D. Yin, *J. Catal.* **2009**, 261, 110; e) B. S. Lane, M. Vogt, V. J. DeRose, K. Burgess, *J. Am. Chem. Soc.* **2002**, 124, 11946; f) J. W. de Boer, W. R. Browne, J. Brinksma, P. L. Alsters, R. Hage, B. L. Feringa, *Inorg. Chem.* **2007**, 46, 6353; g) S. Abdolazadeh, N. M. Boyle, M. Hoogendijk, R. Hage, J. W. de Boer, W. R. Browne, *Dalton Trans.* **2014**, 43, 6322; h) D. A. Valyaev, G. Lavigne, N. Rugan, *Coord. Chem. Rev.* **2016**, 308, 191; i) B. Liua, W. Luoa, H. Li, X. Qi, Q. Hu, *Synth. React. Inorg., Met.-Org., Nano-Met. Chem.* **2015**, 45, 1097; j) T. Katsuki, K. B. Sharpless, *J. Am. Chem. Soc.* **1980**, 102, 5974.
- [10] a) I. Kani, S. Bolat, *Appl. Organomet. Chem.* **2016**, 30(8), 713; b) I. Kani, M. Kurtça, *Turk. J. Chem.* **2012**, 36, 827.
- [11] SMART, **2000**, Bruker AXS
- [12] G. M. Sheldrick, *Acta Crystallogr. Sect. A* **2008**, 64, 112.
- [13] G. M. Sheldrick, SHELXS-97, Program for crystal structure solution. University of Gottingen **1997**.
- [14] C. F. Macrae, P. R. Edgington, P. McCabe, E. Pidcock, G. P. Shields, R. Taylor, M. Towler, J. van de Streek, *J. Appl. Crystallogr.* **2006**, 39, 453.
- [15] A. L. Spek, PLATON - A Multipurpose Crystallographic Tool Utrecht Utrecht University, The Netherlands, **2005**.
- [16] M. J. Frisch, G. W. Trucks, H. B. Schlegel, G. E. Scuseria, M. A. Robb, J. R. Cheeseman, G. Scalmani, V. Barone, B. Mennucci, G. A. Petersson, H. Nakatsuji, M. Caricato, X. Li, H. P. Hratchian, A. F. Izmaylov, J. Bloino, G. Zheng, J. L. Sonnenberg, M. Hada, M. Ehara, K. Toyota, R. Fukuda, J. Hasegawa, M. Ishida, T. Nakajima, Y. Honda, O. Kitao, H. Nakai, T. Vreven, J. A. Montgomery Jr., J. E. Peralta, F. Ogliaro, M. Bearpark, J. J. Heyd, E. Brothers, K. N. Kudin, V. N. Staroverov, T. Keith, R. Kobayashi, J. Normand, K. Raghavachari, A. Rendell, J. C. Burant, S. S. Iyengar, J. Tomasi, M. Cossi, N. Rega, J. M. Millam, M. Klene, J. E. Knox, J. B. Cross, V. Bakken, C. Adamo, J. Jaramillo, R. Gomperts, R. E. Stratmann, O. Yazyev, A. J. Austin, R. Cammi, C. Pomelli, J. W. Ochterski, R. L. Martin, K. Morokuma, V. G. Zakrzewski, G. A. Voth, P. Salvador, J. J. Dannenberg, S. Dapprich, A. D. Daniels, O. Farkas, J. B. Foresman, J. V. Ortiz, J. Cioslowski, D. J. Fox, Gaussian 09, Revision B, Gaussian, Inc., Wallingford CT **2013**.
- [17] a) V. Leyva, I. Corral, T. Schmierer, B. Heinz, F. Feixas, A. Migani, L. Blancafort, P. Gilch, L. Gonzalez, *J. Phys. Chem. A* **2008**, 112, 5046; b) P. Coppens, G. M. J. Schmidt, *Acta Crystallogr.* **1964**, 17, 222.
- [18] A. D. Becke, *J. Chem. Phys.* **1993**, 98, 1372.
- [19] C. T. Lee, W. T. Yang, R. G. Parr, *Phys. Rev. B: Condens. Matter* **1988**, 37, 785.
- [20] K. Nakamoto, *Infrared and Raman Spectra of Inorganic and under investigation. Coordination Compounds*, 4th ed., Wiley, New York **1986** 231.
- [21] a) G. B. Deacon, R. J. Phillips, *Coord. Chem. Rev.* **1980**, 33, 227; b) C. J. Milios, E. Kefalloniti, C. P. Raptopoulou, A. Terzis, A. Escuer, R. Vicente, S. P. Perlepes, *Polyhedron* **2004**, 23, 83.
- [22] J. E. Sheats, R. S. Czernuszewicz, G. C. Dismukes, A. L. Rheingold, V. Petrouleas, J. Stubbe, W. Armstrong, R. H. Beer, S. L. Lippard, *J. Am. Chem. Soc.* **1987**, 109, 1435.
- [23] R. Dingle, *Acta Chem. Scand.* **1966**, 20, 33.
- [24] a) D. Ramalakshmi, M. V. Rajasekharan, *Acta Crystallogr., Sect. B: Struct. Sci.* **1999**, 55, 186; b) C. Wilson, F. K. Larsen, B. N. Figgis, *Acta Crystallogr. Sect. C: Cryst. Struct. Commun.* **1998**, 54, 1797; c) R. Manchanda, G. W. Brudvig, S. de Gala, R. H. Crabtree, *Inorg. Chem.* **1994**, 33, 5157; d) A. F. Jensen, Z. Su, S. K. Hansen, F. K. Larsen, *Inorg. Chem.* **1995**, 34, 4244; e) M. Stebler, A. Ludi, H.-B. Burgi, *Inorg. Chem.* **1986**, 25, 4743; f) P. M. Plaksin, R. C. Stoufer, M. Matthew, G. J. Palenik, *J. Am. Chem. Soc.* **1972**, 94, 2121; g) S. R. Cooper, G. C. Dismukes, M. P. Klein, M. Calvin, *J. Am. Chem. Soc.* **1978**, 100, 7248; h) X. -M. Lu, P. -Z. Li, X. -T. Wang, S. Gao, X. -J. Wang, L. Zhou, C. -S. Liu, X. -N. Sui, J. -H. Feng, Y. -H. Deng,

- Q. -H. Jin, J. Liu, N. Liu, J. -P. Lian, *Polyhedron* **2008**, *27*, 3669; i) D. Kalita, R. Sara, J. B. Baruah, *Inorg. Chem. Commun.* **2009**, *12*, 569; j) R. Wortmann, U. Flörke, B. Sarkar, V. Umamaheshwari, G. Gescheidt, S. Herres-Pawlis, G. Henkel, *Eur. J. Inorg. Chem.* **2011**, 121.
- [25] a) V. Gómez, M. Corbella, M. Font-Bardiab, T. Calvet, *Dalton Trans.* **2010**, *39*, 11664; b) V. Gómez, M. Corbella, F. A. Mautner, O. Roubeau, S. J. Teat, M. Font-Bardia, T. Calvet, *Polyhedron* **2012**, *45*, 185; c) V. Gómez, M. Corbella, *Eur. J. Inorg. Chem.* **2012**, 3147; d) L. Escriche-Tur, M. Corbella, M. Font-Bardia, I. Castro, L. Bonneviot, B. Albelá, *Inorg. Chem.* **2015**, *54*, 10111; e) C. H. L. Kennard, G. Smith, E. J. O'Reilly, W. Chiangjin, *Inorg. Chim. Acta* **1983**, *69*, 53; f) E. Garribba, G. Micera, M. Zema, *Inorg. Chim. Acta* **2004**, 357, 2038; g) T. Glowiak, H. Kozłowski, L. S. Erre, G. Micera, *Inorg. Chim. Acta* **1995**, *236*, 149; h) X. Jiang, H. Liu, B. Zhenga, J. Zhang, *Dalton Trans.* **2009**, 8714; i) J.-J. Zhang, Q.-H. Luo, C.-Y. Duan, Z.-L. Wang, Y.-H. Mei, *J. Inorg. Biochem.* **2001**, *86*, 573.
- [26] a) M. Devereux, M. McCann, V. Leon, V. McKee, R. J. Ball, *Polyhedron* **2002**, *21*, 1063; b) M. D. Godbole, M. Kloskowski, R. Have, A. Rompel, A. M. M. A. L. Spek, E. Bouwman, *Eur. J. Inorg. Chem.* **2005**, 305; c) R. Li, F. Huang, X. Jiang, M. Liu, Y. Song, H. Liu, J. Zhang, *J. Coord. Chem.* **2010**, *63*(9), 1611; d) M. T. Casey, M. McCann, M. Devereux, M. Curran, C. Cardin, M. Convery, V. Quillet, C. Harding, *J. Chem. Soc., Chem. Commun.* **1994**, 2643; e) Y. Naruto, K. Maruyama, *J. Chem. Soc., Chem. Commun.* **1994**, 2667; f) L. Dubois, J. Pcaut, M. F. Charlot, C. Baffert, M. N. Collomb, A. Deronzier, J. M. Latour, *Chem. – Eur. J.* **2008**, *14*, 3013.
- [27] a) S. V. Khangulov, V. V. Barynin, N. V. Voevodskaya, A. I. Grebenko, *Biochim. Biophys. Acta, Bioenerg.* **1990**, *1020*, 305; b) G. S. Waldo, J. E. Penner-Hahn, *Biochemistry* **1995**, *34*, 1507.
- [28] a) K. Wiegardt, U. Bossek, B. Nuber, J. Weiss, J. Bonvoisin, M. Corbella, S. E. Vitols, J. J. Girerd, *J. Am. Chem. Soc.* **1988**, *110*, 7398; b) M. Osawa, U. P. Singh, M. Tanaka, Y. Moro-oka, N. Kitajima, *J. Chem. Soc., Dalton Trans.* **1993**, 310; c) U. P. Singh, R. Singh, S. Hikichi, M. Akita, Y. Morooka, *Inorg. Chim. Acta* **2000**, *310*, 273; d) C. Baffert, M. N. Collomb, A. Deronzier, S. Kjærgaard-Knudsen, J. M. Latour, K. H. Lund, C. J. McKenzie, M. Mortensen, L. P. Nielsen, N. Thorup, *Dalton Trans.* **2003**, 1765; e) M. U. Triller, W. Y. Hsieh, V. L. Pecoraro, A. Rompel, B. Krebs, *Inorg. Chem.* **2002**, *41*, 5544; f) S. Signorella, A. Rompel, K. B. Karentzopoulos, B. Krebs, V. L. Pecoraro, *Inorg. Chem.* **2007**, *46*, 10864.
- [29] a) M. Bagherzadeh, A. Ghanbarpour, H. R. Khavasi, *Catal. Commun.* **2015**, *65*, 72; b) H. R. Khavasi, K. Sasan, M. Pirouzmand, S. N. Ebrajimi, *Inorg. Chem.* **2009**, *48*, 5593; c) S. T. Castamana, S. Nakagaki, R. R. Ribeiroa, K. J. Ciuffib, S. M. Drechsel, *J. Mol. Catal. A: Chem.* **2009**, *300*, 89; d) M. Louloui, C. Kolokytha, N. Hadjiliadis, *J. Mol. Catal. A: Chem.* **2002**, *180*, 19; e) G. B. Shul'pin, G. Süß-Fink, L. S. Shul'pina, *J. Mol. Catal. A: Chem.* **2001**, *170*, 17; f) J. Rich, E. Manrique, F. Molton, C. Duboc, M.-N. Collomb, M. Rodríguez, I. Romero, *Eur. J. Inorg. Chem.* **2014**, 2663; g) G. B. Shul'pin, G. V. Nizova, Y. N. Kozlov, I. G. Pechenkina, *New J. Chem.* **2002**, *26*, 1238.

SUPPORTING INFORMATION

Additional Supporting Information may be found online in the supporting information tab for this article.

How to cite this article: Su E, Guven A, Kani I. Oxygen bridged Homobinuclear Mn(II) compounds with Anthranilic acid: Theoretical calculations, oxidation and catalase activity. *Appl Organometal Chem.* 2017;e4105. <https://doi.org/10.1002/aoc.4105>

APPENDIX A

CCDC 1458044 and 827685 contain the supplementary crystallographic data for $[\text{Mn}_2(\mu\text{-}2\text{-NH}_2\text{C}_6\text{H}_4\text{COO})_2(\text{phen})_4](\text{ClO}_4)_2(\text{CH}_3\text{OH})$ (**1**) and $[\text{Mn}_2(\mu\text{-}2\text{-NH}_2\text{C}_6\text{H}_4\text{COO})_2(\text{bipy})_4](\text{ClO}_4)_2$ (**2**). These data can be obtained free of charge via <http://www.ccdc.ac.uk/conts/retrieving.html>, or from the Cambridge Crystallographic Data Centre, 12 Union Road, Cambridge CB2 1EZ, UK; fax: (+44) 1223-336-033; or Email: deposit@ccdc.cam.ac.uk.